# Indian Ocean variability changes in PMIP4

Chris Brierley[1], Kaustubh Thirumalai[2], and Edward Grindrod[3]

[1]Dept. Geography, University College London, London, United Kingdom
[2]Dept. Geosciences, University of Arizona, Tucson, Arizona, USA

**Correspondence:** Chris Brierley (c.brierley@ucl.ac.uk)

**Abstract.** TEXT



## 1 Introduction

- Introduce Indian Ocean and its importance
- Variability in the Indian Ocean
- past climates in general, and PMIP specifically
- past knowledge of variability
  - literature on paleoIOD
  - literature on IOBM (not much at all)
  - literature on Nino mode

| Model | piControl | historical | midHolocene | lgm | lig127k | 1pctCO2 | abrupt4xCO2 |
|---|---|---|---|---|---|---|---|
| ACCESS-ESM1-5 | 100 | 165 | - | - | 200 | 150 | - |
| AWI-ESM-1-1-LR | 100 | 165 | 100 | 100 | 100 | - | - |
| BCC-CSM1-1 | 500 | 163 | 100 | - | - | 140 | 150 |
| CCSM4 | 1051 | 156 | 301 | 101 | - | 156 | 151 |
| CESM2 | 500 | 165 | 700 | - | 700 | 150 | 150 |
| CNRM-CM5 | 850 | 156 | 200 | 200 | - | 140 | 150 |
| CNRM-CM6-1 | 500 | 165 | - | - | 301 | 150 | 150 |
| COSMOS-ASO | 400 | - | - | 600 | - | - | - |
| CSIRO-Mk3-6-0 | 500 | 156 | 100 | - | - | 140 | 150 |
| CSIRO-Mk3L-1-2 | 1000 | 150 | 500 | - | - | 140 | - |
| EC-Earth3-LR | 201 | - | 201 | - | - | - | - |
| FGOALS-f3-L | 561 | 165 | 200 | - | 500 | 160 | 160 |
| FGOALS-g2 | 700 | 115 | 680 | 100 | - | 244 | 258 |
| FGOALS-g3 | 500 | - | 500 | - | 500 | - | - |
| FGOALS-s2 | 501 | - | 100 | - | - | 140 | 150 |
| GISS-E2-1-G | 851 | 165 | 100 | - | 100 | 51 | 151 |
| t GISS-E2-R | 500 | 156 | 100 | 100 | - | 151 | 151 |
| HadGEM2-CC | 240 | 145 | 35 | - | - | - | - |
| HadGEM2-ES | 336 | 145 | 101 | - | - | 140 | 151 |
| HadGEM3-GC31-LL | 100 | 165 | 100 | - | - | - | - |
| INM-CM4-8 | 531 | 165 | 200 | 200 | 100 | 150 | 150 |
| IPSL-CM5A-LR | 1000 | 156 | 500 | 200 | - | 140 | 260 |
| IPSL-CM6A-LR | 1200 | 165 | 550 | - | 550 | 150 | 900 |
| KCM1-2-2 | 200 | - | 100 | - | - | - | - |
| MIROC-ES2L | 500 | 165 | 100 | 100 | 100 | 150 | 150 |
| MIROC-ESM | 630 | 156 | 100 | 100 | - | 140 | 150 |
| MPI-ESM-P | 1156 | 156 | 100 | 100 | - | 140 | 150 |
| MPI-ESM1-2-LR | 1000 | 165 | 500 | 100 | 300 | 165 | 165 |
| MRI-CGCM3 | 500 | 156 | 100 | 100 | - | 140 | 150 |
| MRI-ESM2-0 | 701 | 165 | 200 | - | - | 151 | 151 |
| NESM3 | 100 | 165 | 100 | - | 100 | 150 | 150 |
| NorESM1-F | 200 | - | 200 | - | 200 | - | - |
| NorESM2-LM | 391 | 65 | 100 | - | 100 | 30 | 380 |
| UofT-CCSM-4 | 100 | - | 100 | 100 | - | - | - |

**Table 1.** The number of years of data for iod timeseries mon in the CVDP archive

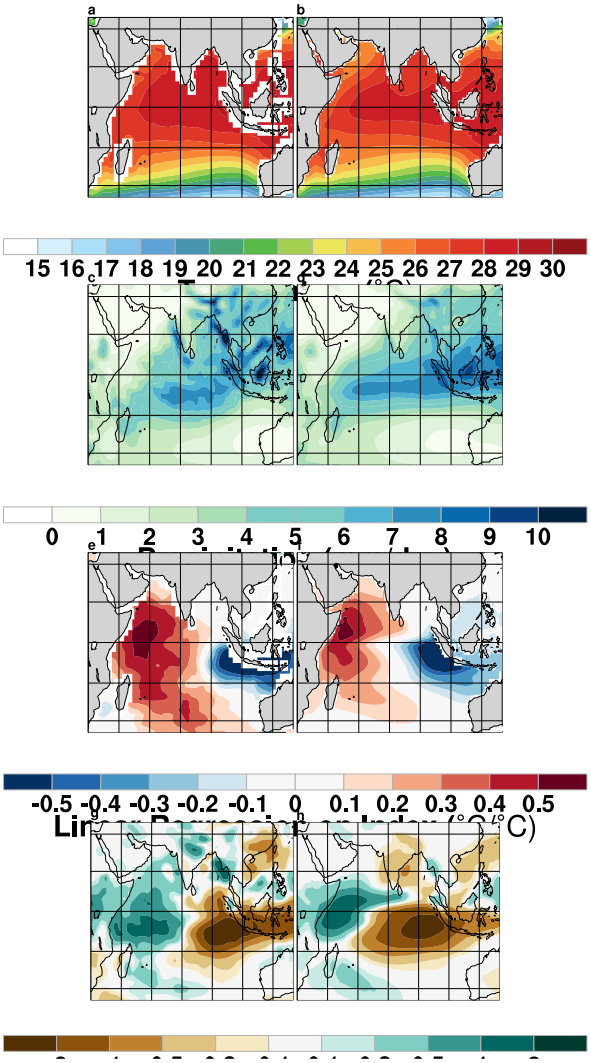


**Figure 1. Comparison between the observed climate and the PMIP ensemble**. The left hand side is taken from the 20th Century Re-analysis (**?**), with the ensemble mean of the preindustrial control simulations on the right. The rows present the annual mean sea surface temperatures (a,b), annual mean precipitation (c,d), IOD pattern computed by regressing the monthly SST anomalies against the DMI (e,f; sec. 2.3) and the rainfall anomalies associated with IOD variations (g,h).

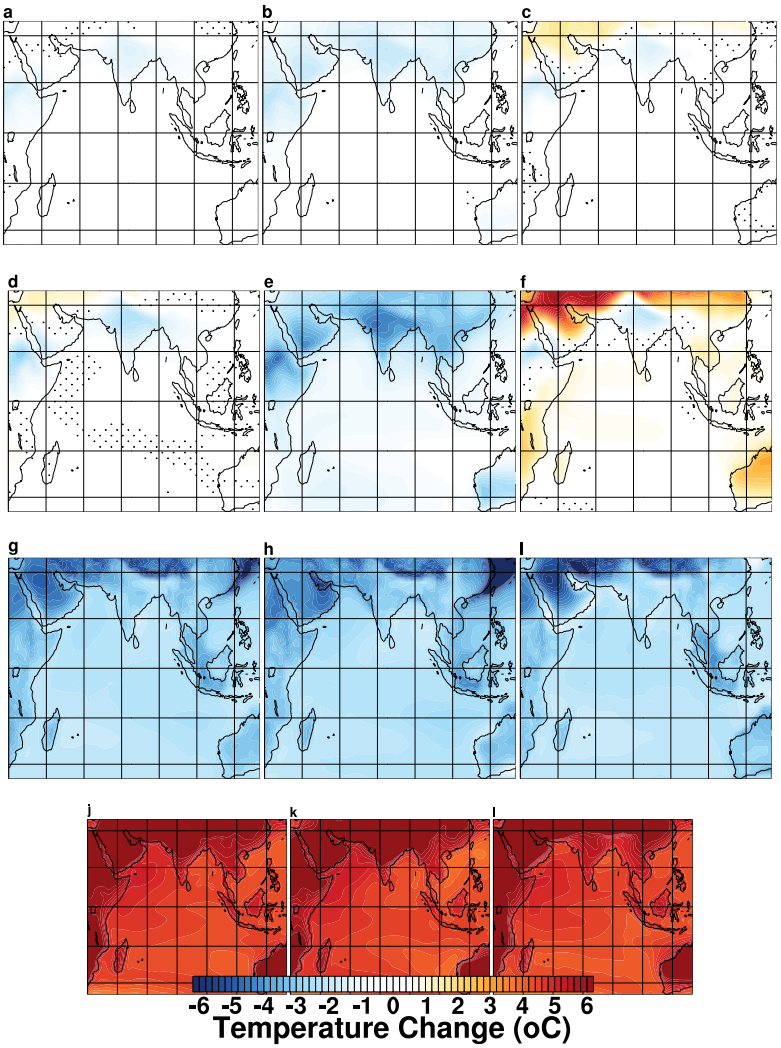


**Figure 2. Ensemble mean change in surface temperatures**. The columns show the annual mean (a,d,g,j), DJF (b,e,h,k) and JJA (c,f,i,l). The rows show the ensemble mean difference from the piControl simulations for the midHolocene (a,b,c), lig127k (d,e,f), lgm (g,h,i) and abrupt4xCO2 simulations (j,k,l). Stippling indicates where the ensemble is not consistent in the direction of change.

## 2 Methods

### 2.1 Models

### 2.2 Experiments

### 2.3 Analysis and definitions



## 3 Results

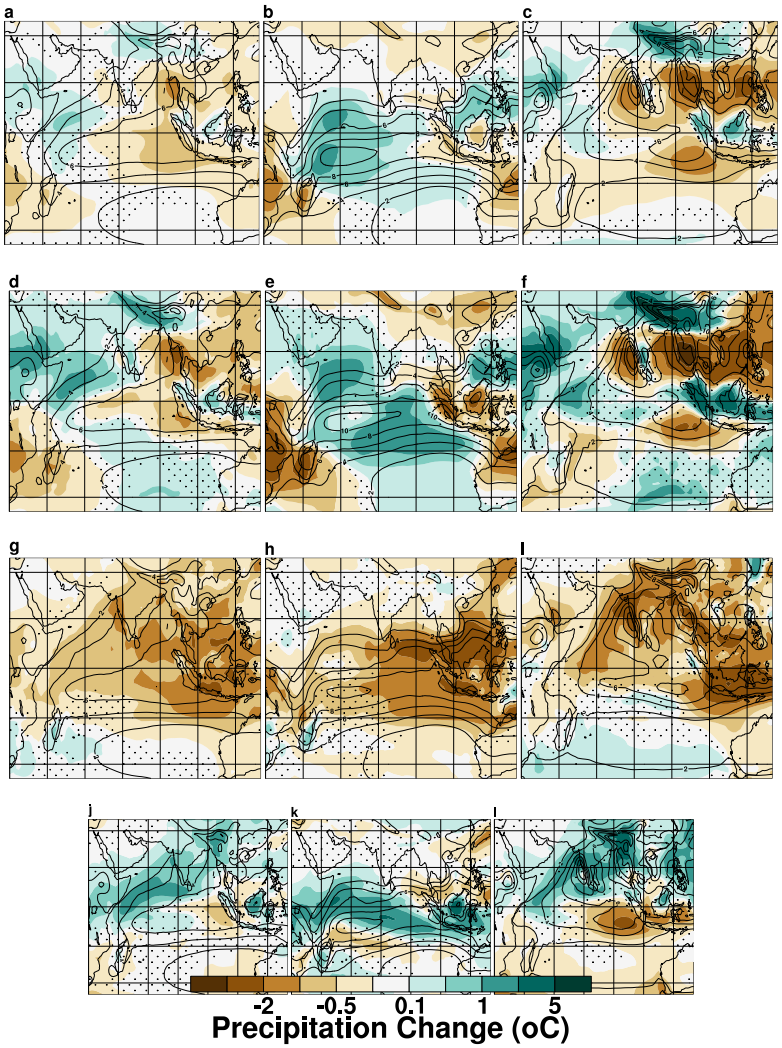


**Figure 3. Ensemble mean change in precipitation**. The columns show the annual mean (a,d,g,j), DJF (b,e,h,k) and JJA (c,f,i,l). The rows show the ensemble mean difference from the piControl simulations for the midHolocene (a,b,c), lig127k (d,e,f), lgm (g,h,i) and abrupt4xCO2 simulations (j,k,l). Stippling indicates where the ensemble is not consistent in the direction of change.

*Author contributions.* TEXT

*Competing interests.* TEXT

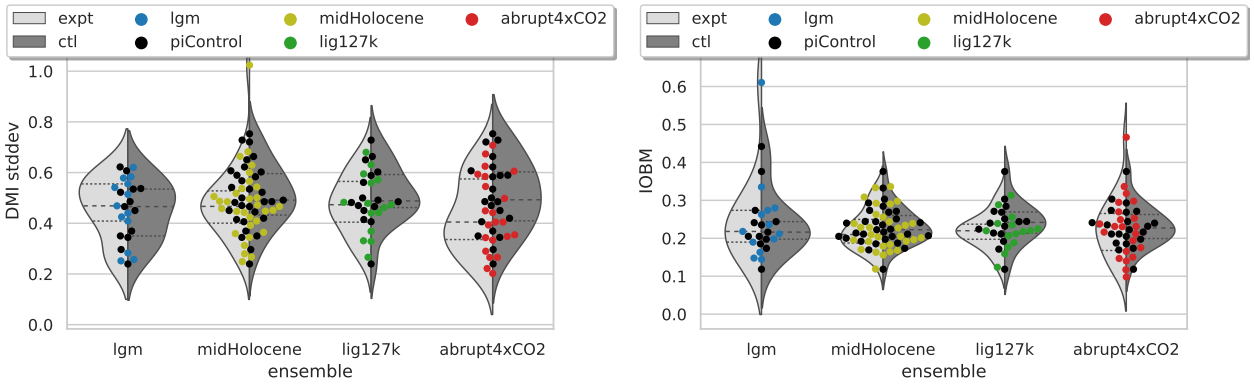


**Figure 4. Amplitude changes in modes of Indian Ocean variability**. (a) The amplitude of the Indian Ocean dipole is measured by standard deviation of the dipole mode index (DMI, sec. 2.3). (b) The amplitude of the Indian Ocean basin mode (IOBM) is measured by the standard deviation of the tropical Indian Ocean index (see sec. 2.3 for definition).

*Disclaimer.* TEXT

*Acknowledgements.* TEXT

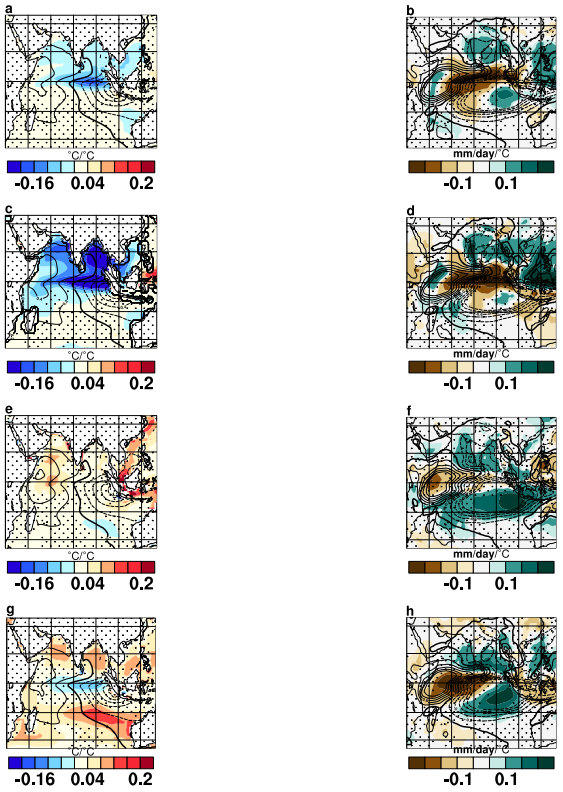


**Figure 5. Ensemble mean change in SST and rainfall patterns of the Indian Ocean dipole**. Each row represents the ensemble mean difference from the piControl simulations a different experiment; with the midHolocene changes in SST (a) and rainfall (b), the lig127k changes in SST (c) and rainfall (d), the lgm changes in SST (e) and rainfall (f), and the abrupt4xCO2 changes in SST (g) and rainfall (h) patterns respectively. Stippling indicates where the ensemble is not consistent in the direction of change. The overlaid contours show the ensemble mean pattern in the piControl simulations, with dashed contours indicate negative numbers. As the models contributing to each experiment changes, so does the precise pattern of piControl patterns.

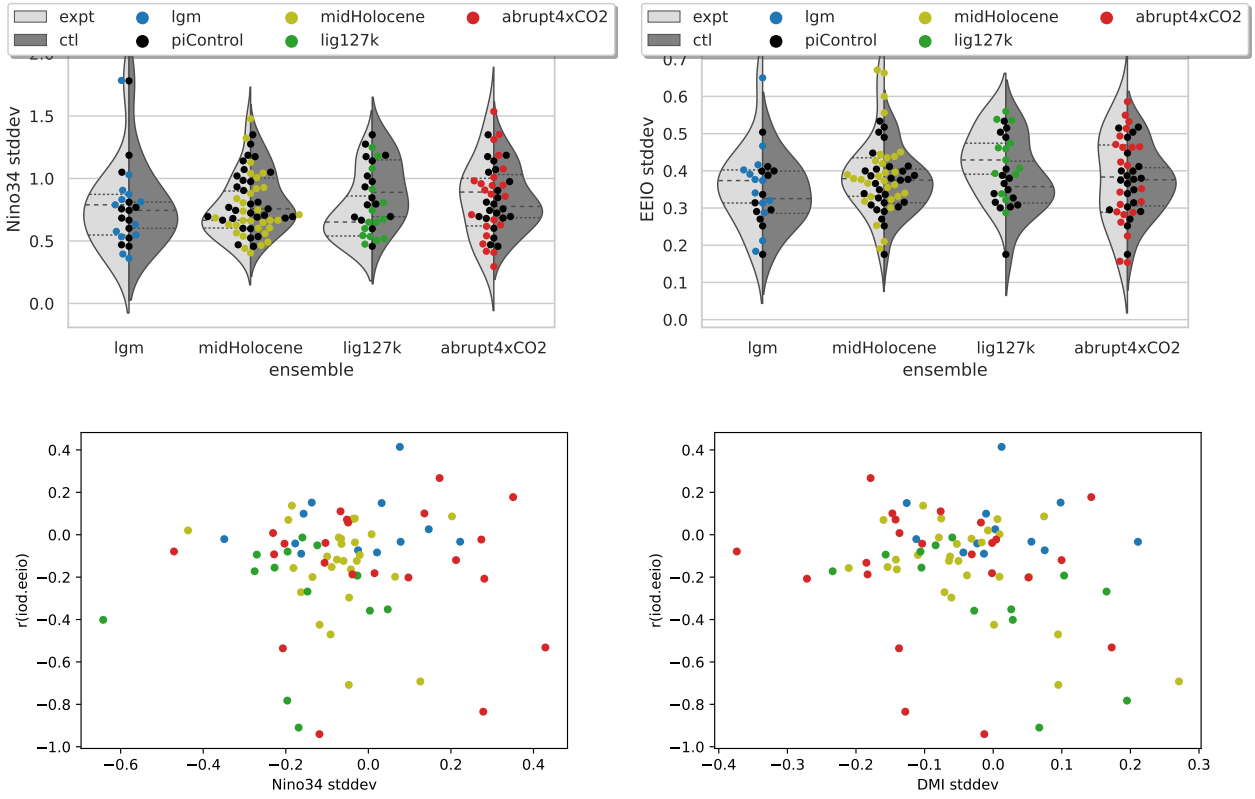


**Figure 6. Response of Niño modes**. (a) The amplitude of Pacific ENSO is measured by standard deviation of the Niño3.4 SST anomalies (sec. 2.3). (b) The amplitude of the Indian Ocean Niño-like mode is measured by the standard deviation of the eastern equatorial Indian Ocean SST anomalies (see sec. 2.3 for definition). (c) The changes in the correlation correlation coefficient between the two Niño modes, as a function of changes in the amplitude of Pacific ENSO. (d) The changes in the correlation correlation coefficient between the Indian Ocean dipole and the Indian Ocean Niño-like mode, as a function of changes in the amplitude of the Indian Ocean dipole.

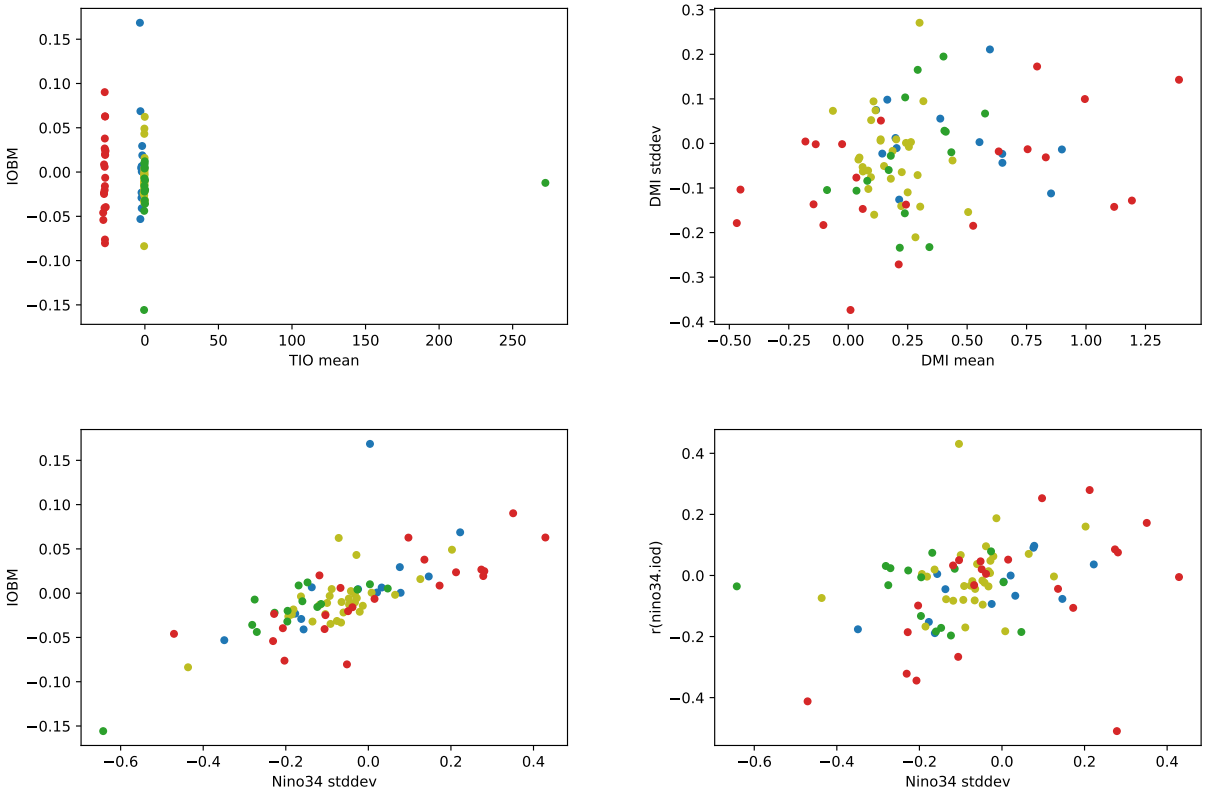


**Figure 7. Relationships between the amplitude changes in modes of Indian Ocean variability and the mean state**. (a) The amplitude of the Indian Ocean basin mode does not respond to changes in the tropical Indina Ocean SST. (b) The amplitude of the Indian Ocean dipole mode does not exhibit a simple linear relationship with changes in the zonal gradient. (c) Amplitude changes of the IOBM are linearly related to changes in ENSO amplitude. (d) There is a weak indication at that ENSO amplitude becomes larger, its correlation with the IOD also strengthens.